SIMULATION OF CONSTRUCTION OF RCC DAMS. II: STRESS AND DAMAGE

By Miguel Cervera,[1] Javier Oliver,[2] and Tomás Prato[3]

ABSTRACT: The increasing number of roller compacted concrete (RCC) dams being built around the world demands accurate methodologies for the realistic short- and long-term evaluations of the risk of thermally induced cracking in these constructions. In this work a numerical procedure for the simulation of the construction process of RCC dams is presented. It takes into account the more relevant features of the behavior of concrete at early ages, such as hydration, aging, creep, and damage. A 2D model of the Urugua-í RCC Dam, built in Argentina, is used to perform the corresponding analyses. In this second part of the paper, the mechanical aspects of the simulation are presented; long-term effects are included by incorporating a creep model that naturally accounts for the aging effects, and the risk of tensile damage is also considered. The methodology determines the stress field inside the dam at any time during the construction and in the following years. Results for the reference case assess the suitability of the adopted design. This is compared to alternative studies considering different construction schedules to conclude that for these cases changes should be introduced in the dam design.

INTRODUCTION AND MOTIVATION

The basic design requirement for concrete dams is to ensure their integrity, watertightness, and durability. Therefore, any new procedure for dam construction must contemplate and adopt measures against the risk of cracking, and, in particular, against thermally induced cracking. This is also the case for roller compacted concrete (RCC) dams, where, to achieve the high production rates that make them economically profitable, longitudinal joints are totally avoided, pipe cooling is not suitable, and even transverse joints must be reduced to a minimum. Because of this, the technological specifications for massive concrete dams differ from those used for slim structures in one essential point: heat generation and the resulting thermal stresses are decisive, rather than attaining a high initial strength.

One of the main features of RCC is that its low cement content makes its hydration heat comparatively low, up to three times smaller than for conventional concretes. Nevertheless, the high concreting rate used in RCC dams may lead to significant temperature rises [see Part I (Cervera et al. 2000)]. This increase in temperature occurs during the first days after placing, when the stiffness of concrete is still quite low and creep (viscous) effects are significant; therefore, it usually leads to moderate, and mainly compressive, stresses. This means that, in general, the dam may be considered as virtually free from thermally induced tensile stresses at the moment of completion.

However, months later, when the hydration process has finished, no more hydration heat is produced; the stiffness has significantly increased, and the concrete starts to cool down. The temperature in the body of the dam drops from the (almost) maximum values attained at the completion of the construction process to a finally stable distribution that will consist of seasonal oscillations around the mean annual temperature.

The drop in the temperature at a point is inevitably accompanied by a volume reduction. If this volume change is restricted by the surrounding concrete or the foundation rock, thermally induced stresses will develop and may lead to cracking. Therefore, the cause of thermal stresses and cracking is not the temperature change in itself, but the spatial restriction for free thermal shrinkage.

The main causes for volume change restriction are

- The nonuniform temperature distribution due to the evolutionary construction process
- Thermal gradients near the faces of the dam due to convection phenomena with the environment
- External geometrical and thermal restraints such as the foundation rock
- Design geometrical aspects such as the distance between transverse joints

Therefore, the investigation of the risk of cracking due to thermal variation must distinguish two main different patterns:

- Cracking in the interior of the dam body due to the cooling process from the nonuniform distribution of maximum temperatures down to the mean annual temperature—This cooling process may take several years after the completion of the dam.
- Cracking near the surface as a consequence of the thermal gradient in concrete—This gradient increases, for instance, with the fast surface cooling due to the ambient air temperature. This process may become the critical problem during the first weeks after concreting.

This paper presents a numerical procedure for the simulation of the construction process of RCC dams. First, a mechanical model is proposed to predict the evolution of the thermally induced stresses in concrete at early ages. The reference model is based on the theory of continuum damage mechanics, and it incorporates two separate scalar internal variables to represent damage under tension and compression conditions. The damage model is reformulated in a suitable normalized format so that it can incorporate the phenomenon of aging. Long-term mechanical behavior is considered by incorporating a creep model inspired in the recently proposed Microprestress-Solidification Theory. Second, the case study of Urugua-í RCC Dam in Argentina is discussed. The stress analysis during the construction and the first 11 years of service life of the dam is carried out. Results concerning the short-term, long-term, and stable regimes are shown to assess the safety of the design and the risk of tensile cracking. Third, alternative stud-

[1]Prof. Struct. Mech., ETS Ingenieros de Caminos, 08034 Barcelona, Spain.
[2]Prof. Continuum Mech., ETS Ingenieros de Caminos, 08034 Barcelona, Spain.
[3]Grad. Res. Asst., ETS Ingenieros de Caminos, 08034 Barcelona, Spain.

Note. Associate Editor: Walter H. Gerstle. Discussion open until February 1, 2001. Separate discussions should be submitted for the individual papers in this symposium. To extend the closing date one month, a written request must be filed with the ASCE Manager of Journals. The manuscript for this paper was submitted for review and possible publication on March 17, 1999. This paper is part of the ***Journal of Structural Engineering***, Vol. 126, No. 9, September, 2000. ©ASCE, ISSN 0733-9445/00/0009-1062–1069/$8.00 + $.50 per page. Paper No. 20475.

ies considering different construction schedules are performed to evaluate their effect on the safety assessment of the dam.

NUMERICAL MODEL

The long-term mechanical behavior of concrete under sustained loading necessarily involves the consideration of creep phenomena. These are particularly significant if the stress analysis includes the simulation of the construction process, as rheological effects are most evident for early age concrete. Also, failure under tensile stresses must be considered if the goal of the stress analysis is to assess the risk of cracking. To this end, modeling in a realistic manner the mechanisms through which (tensile) strength and stiffness develop in the material at early ages is of great importance. The mechanical model used in this work is described in detail in Cervera et al. (1999), and it will only be sketched here. It combines the use of up-to-date aging and viscoelastic and damage models to provide a phenomenological description of the mechanical behavior of early age concrete that can be used for engineering purposes. The assessment of the model and relevant numerical simulations of available experiments can also be found in that reference.

Microprestress-Solidification Theory

Undoubtedly, one of the most widely accepted models for creep in early age concrete is the so-called Solidification Theory, developed and refined over the last 25 years [Bazant (1979), Bazant and Prasannan (1989), and Bazant et al. (1997), among others]. The basic idea behind this theory is to consider concrete as a viscoelastic material that can be interpreted as a generalized Kelvin chain with a series arrangement. The different elastic moduli present in the chain vary in time proportionally and are governed by the value attained by a proposed ''solidified fraction.'' The present model follows closely the latest developments in Solidification Theory but is applied to a basic viscoelastic material that is interpreted as a generalized Maxwell chain with a parallel arrangement. This modification leads to significant computational advantages, as pointed out in Carol and Bazant (1993) and Cervera et al. (1999).

Fig. 1 shows a schematic representation of the viscoelastic rheological model used to represent the long-term mechanical behavior of concrete; it consists of a generalized Maxwell model that can be described in terms of the elastic moduli of the springs E^i and the relaxation times of the dashpots τ^i of the $i = 1, \ldots, N$ Maxwell elements of the chain. The volumetric strain due to thermal effects is represented in Fig. 1 by the circular element connected in series to the chain arrangement. We will assume that during the aging process all of the elastic moduli vary proportionally to the aging function defined by the aging model (see Part I), $E^i(\kappa) = \kappa^{1/2} E^i_\infty$ (where κ is the aging degree and E^i_∞ is the value at the end of the hydration process), and that the relaxation times remain constant.

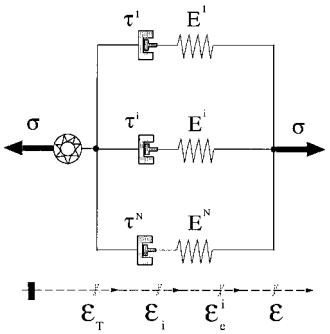

FIG. 1. Rheological Model for Long-Term Behavior

Being a parallel arrangement, the total stress sustained by the Maxwell chain is

$$\boldsymbol{\sigma} = \sum_{i=1}^{N} \bar{\boldsymbol{\sigma}}^i \tag{1}$$

where $\bar{\boldsymbol{\sigma}}^i$ = (elastic) stress in each Maxwell element of the chain. Note that multiaxial models tensor entities (in boldface) are simply the multidimensional counterparts of the scalar ones used for uniaxial models. It was shown in Cervera et al. (1999) that these stresses can be computed as

$$\bar{\boldsymbol{\sigma}}^i = \mathbf{D}^i(\kappa)(\boldsymbol{\varepsilon} - \boldsymbol{\varepsilon}_T - \boldsymbol{\varepsilon}^i) = \mathbf{D}^i(\kappa)\boldsymbol{\varepsilon}^i_e \quad \text{for } i = 1, \ldots, N \tag{2}$$

where $\mathbf{D}^i(\kappa)$ = elastic constitutive tensor computed in terms of the corresponding current elastic moduli $E^i = E^i(\kappa)$; and $\boldsymbol{\varepsilon}^i_e$ = elastic strain in each Maxwell element. Note that these elastic strains are defined in terms of the total strain $\boldsymbol{\varepsilon}$, the volumetric thermal strain $\boldsymbol{\varepsilon}_T$, and the viscous strain in each Maxwell element $\boldsymbol{\varepsilon}^i$.

The thermal volumetric strain can be defined in terms of the temperature T and the thermal expansion coefficient α_T in the usual way

$$\boldsymbol{\varepsilon}_T = \alpha_T(T - T_{\text{ref}})\mathbf{1} \tag{3}$$

with the reference temperature T_{ref} taken as equal to the temperature reached at the end of the setting phase (when the hydration degree reaches the percolation threshold, $\xi = \xi_{\text{set}}$).

The evolution of the viscous strains can be computed as

$$\dot{\boldsymbol{\varepsilon}}^i = \left(\frac{1}{\tau^i} + \frac{1}{\tau_a}\right)\boldsymbol{\varepsilon}^i_e \quad \text{for } i = 1, \ldots, N \tag{4}$$

with $\tau_a(\kappa) = 2\kappa/\dot{\kappa}$ representing the aging effect on the elastic modulus. Note that when the hydration process is completed $\dot{\kappa}$ vanishes, and the model reverts to a standard Maxwell viscoelastic arrangement.

However, experimental evidence shows that the phenomenon of creep under fixed sustained load decreases significantly with the age at loading even after many years, whereas the hydration reaction is practically completed after 1 year of age. This very long-term nonlinear effect is taken into account in the solidification theory by supplementing the serial Kelvin chain with an additional dashpot with a time-dependent viscosity. In Bazant et al. (1997) a physical model is formulated to obtain the viscosity of this dashpot as a function of the tensile micro-prestress carried by the bonds and bridges crossing the gel pores in the hardened cement gel. The long-term creep is assumed to originate from viscous shear slips between the opposite walls of micropores in which the bonds that transmit the micro-prestress break and reform. In Cervera et al. (1999) this nonlinear viscous effect is included in the parallel Maxwell chain by modifying (4) in the form

$$\dot{\boldsymbol{\varepsilon}}^i = \left(\frac{1}{\tau^i} + \frac{1}{\tau_a} + \frac{1}{\tau_\mu}\right)\boldsymbol{\varepsilon}^i_e \quad \text{for } i = 1, \ldots, N \tag{5}$$

where τ_μ = relaxation time of the additional creep mechanism. If humidity effects are not considered, the evolution of this can be expressed as a function of time

$$\tau_\mu = \frac{\tau_{\mu 0}(1 + c_{\mu 0} t)}{\kappa^{1/2}} \tag{6}$$

where $\tau_{\mu 0}$ and $c_{\mu 0}$ = material properties. Note that, as time increases, τ_μ will tend to infinity, and the flow term will eventually become inactive.

Aging Viscoelasticity and Damage

Finally, let us consider the coupling of the aging viscoelastic model described above with the aging damage model de-

scribed in Cervera et al. (1999). To this end, let us find the value of the principal stresses, distinguish their tensile (positive) from the compressive (negative) values, and define the following split of the elastic stresses for each element in the chain

$$\bar{\boldsymbol{\sigma}}^{i} = \bar{\boldsymbol{\sigma}}^{i+} + \bar{\boldsymbol{\sigma}}^{i-} \tag{7}$$

where $\bar{\boldsymbol{\sigma}}^{i+}$ = elastic tensile stress; and $\bar{\boldsymbol{\sigma}}^{i-}$ = elastic compressive stress.

Eq. (1), which gives the total stress sustained by the Maxwell chain, is now replaced by the expression

$$\boldsymbol{\sigma} = (1 - d^{+}) \sum_{i=1}^{N} \bar{\boldsymbol{\sigma}}^{i+} + (1 - d^{-}) \sum_{i=1}^{N} \bar{\boldsymbol{\sigma}}^{i-}$$

$$= (1 - d^{+})\bar{\boldsymbol{\sigma}}^{+} + (1 - d^{-})\bar{\boldsymbol{\sigma}}^{-} \tag{8}$$

where the damage indices under tension and compression, d^{+} and d^{-}, respectively, have been introduced.

The damage indices are equal to zero for (elastic) undamaged concrete. Concrete remains undamaged as long as the total tensile and compressive elastic stresses do not exceed the corresponding tensile or compressive strengths. For early age concrete these strengths depend on the progress of the hydration reaction through the aging degree (see Part I). Under increasing loading the damage indices are monotonically increasing functions of the corresponding stresses, varying in the range of $0 \leq d^{+}(\bar{\boldsymbol{\sigma}}^{+})$, and $d^{-}(\bar{\boldsymbol{\sigma}}^{-}) \leq 1$.

The detailed description of the procedures followed for the characterization and evolution of the damage indices is given in Cervera et al. (1999).

URUGUA-Í DAM

A brief description of the Urugua-í Dam project is given in Part I of this work. The reader may refer to it for details about the geometry of the dam as well as the material properties of the four different types of concrete used in the foundation, body, and faces.

The 2D finite-element model used to perform the thermal analysis of the actual evolutionary construction process of the dam is also described in Part I. The same discrete model will be used in the next section to perform the stress analysis, as well as some additional studies related to alternative construction schedules. Therefore, the reader may refer to it for details about the finite-element discretization and the procedure for progressively activating the different concrete lifts at the times corresponding to their respective placing in the dam.

STRESS ANALYSIS

In this section, results from thermally induced stress analyses performed on a numerical model of Urugua-í RCC Dam are presented. First, results from the reference case study, simulating the real construction process of the dam are discussed. This will provide the assessment of the dam design and the actual short- and long-term safety conditions of the construction. Second, the analysis is repeated simulating a 3-month interruption of the construction process during the winter. The impact of such eventuality is studied, and the comparison with the reference case is described. Third, the analysis is repeated under the hypothesis that the placement interval is doubled, and, therefore, the construction process is completed in 2 years. Again, results are compared to those from the reference case.

Reference Case Study

The reference case study corresponds to the actual concreting program followed in the construction process of the Urugua-í RCC Dam. Concreting of the foundation began in January 1988, in the middle of the austral summer, and was completed in March of the same year. The placing of RCC began in April 1988 and was finished in March 1989. Therefore, it can be considered that the construction of the body of the dam took approximately 1 year. The dam was built with 40-cm-thick lifts. The placement interval between lifts was approximately 48 h. Therefore, the placing speed can be estimated as $V = 20$ cm/day. The time step used in the analysis during the construction of the dam is 12 h, so that once a lift is activated four time steps pass before a new lift is placed above.

Fig. 2 shows the short-term (during construction) longitudinal stress evolution for interior points located at different elevations. The corresponding (placing months) elevations are (April) 130 m, (June) 141 m, (August) 153 m, (October) 165 m, and (December) 177 m. Note that June to August correspond to the austral winter season, and December to February correspond to austral summer. As the placing temperature is assumed to be higher than the ambient temperature (+5°C), the lifts start to cool after being placed, and they go into tension because of the restriction to deform imposed by the lifts below. However, the stress turns into compression shortly afterward, as the concrete starts to warm because of the release of the hydration heat and the heat flux coming from the surrounding concrete. This lasts until the concrete begins to cool again after the hydration process is finished, and the heat in the dam is released toward the environment and the foundation rock. Note that lifts placed at the bottom of the dam begin to cool fairly early after their placement, and they are subjected to tension almost from the beginning (self-weight not considered).

Fig. 3 shows the long-term (after completion) stress evolution for the same interior points monitored in Fig. 2. The stress analysis was run for 11 years after completion of the dam. During this period the temperature in the interior of

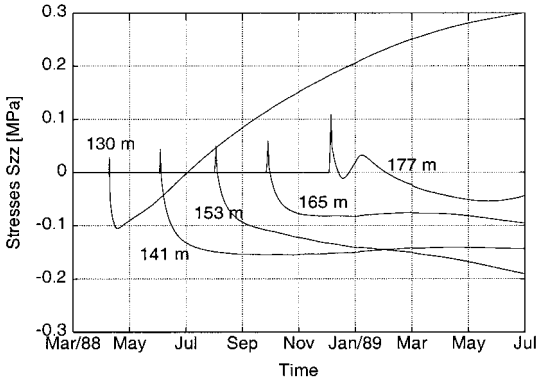

FIG. 2. Short-Term Stress Evolution for Different Elevations

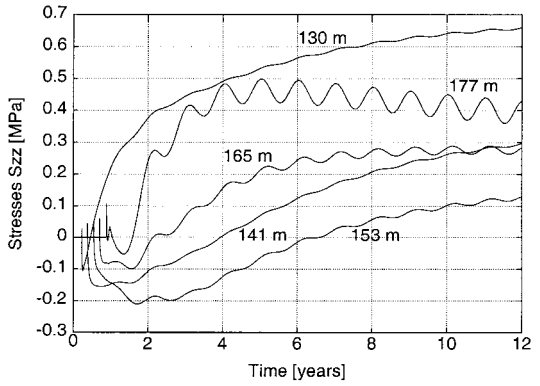

FIG. 3. Long-Term Stress Evolution for Different Elevations

the dam decreases progressively, as the heat generated during the hydration process is released through the upstream and downstream faces. The final stable temperature in the interior of the dam will be approximately equal to the mean annual temperature (20°C). As the temperature drops, the longitudinal stress in concrete turns progressively from compression to tension. This phenomenon is faster for the upper elevations, because they were placed in the summer and because they are more exposed to the ambient temperature. However, the bottom lifts also go into tension very quickly because of the loss of heat toward the foundation rock. Note also that the seasonal oscillation of the ambient temperature is only noted in the stresses for the points located at higher elevations, whereas the bottom part of the dam body is virtually unaffected by it.

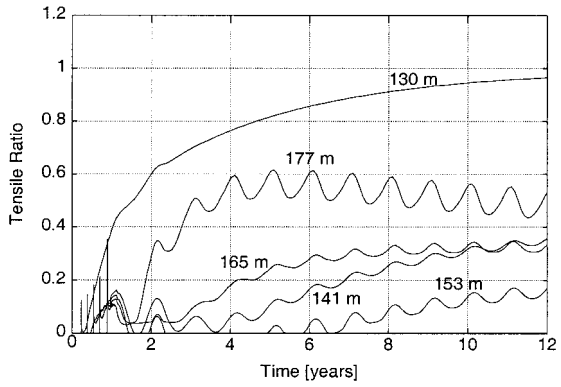

FIG. 4. Long-Term Tensile Ratio Evolution for Different Elevations

The evolution of the long-term tensile stresses must be compared with the development of the tensile strength, in order to assess the risk of cracking. Note that different tensile strengths are attained at the different elevations, due to the influence of temperature in the aging process. Fig. 4 combines both results by showing the evolution of the tensile ratio, defined as the ratio of (the norm of) the tensile stresses over the current tensile strength. The closer this value is to unity, the greater is the risk of the onset of tensile damage. The present analysis shows significant risk of tensile cracking in the long term in the contact area between the dam and the foundation (Elevation 125 m). This risk is well recognized in the literature, and it is usually referred to as cracking by external restraint. In fact, the stress analysis performed for Miyagase RCC Dam, reported by Hirose et al. (1988), found that the maximum risk of cracking occurred when the concrete just above the foundation rock was placed in summer. Nevertheless, it must be remarked that, due to Poisson's effect, the compressive vertical stresses due to self-weight will also lead to compressive longitudinal stresses that largely reduce the risk of tensile cracking in this bottom area.

Tensile straining in areas located well above the foundation is caused by the internal restraint originated by nonuniform temperature distribution and evolution inside the dam. In general, it can be concluded from the data in Figs. 3 and 4 that, away from the foundation, the higher the location, the greater the risk of tensile damage due to internal restraint. This was

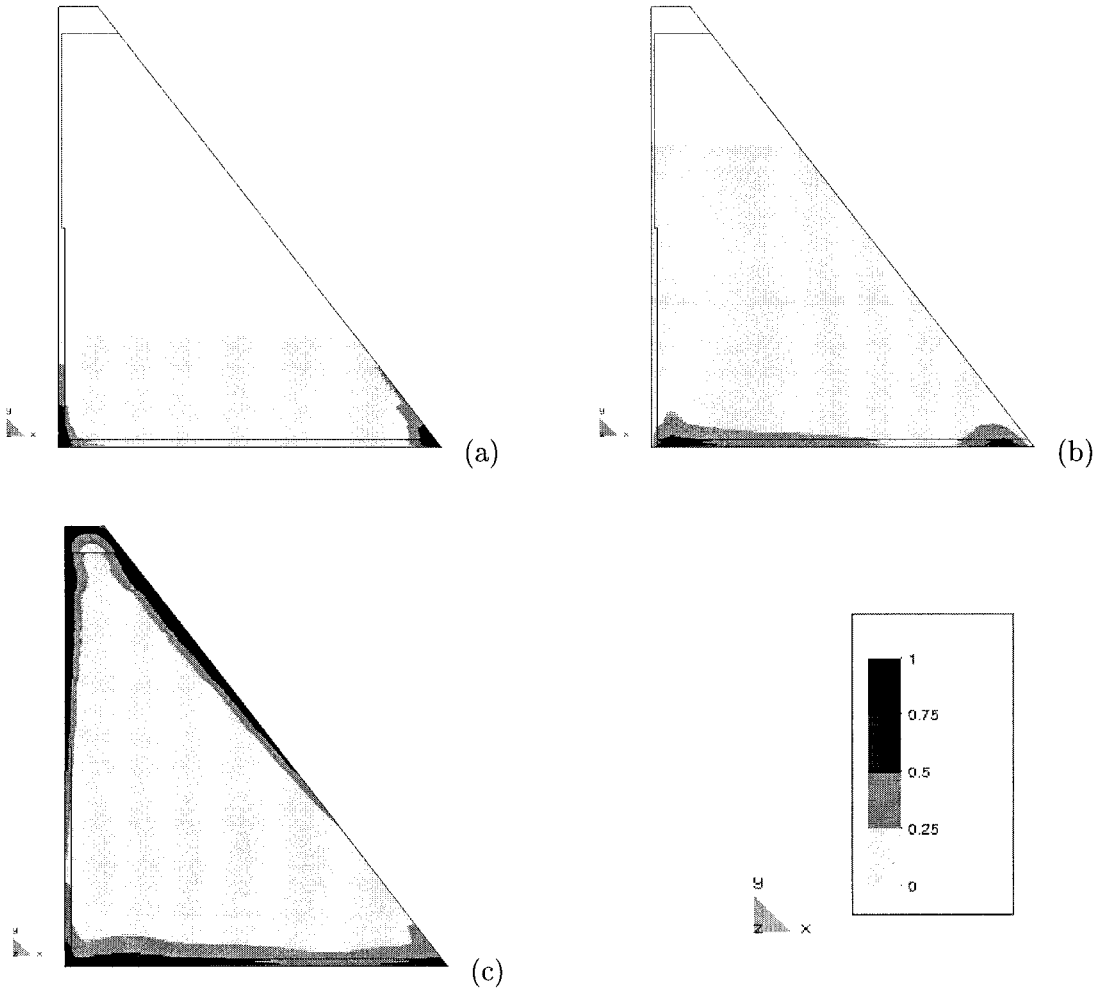

FIG. 5. Short-Term Evolution of Tensile Ratio; Corresponding (Months) Elevations Are: (a) (June 1988) 146 m; (b) (November 1988) 175 m; (c) (June 1989) 196 m

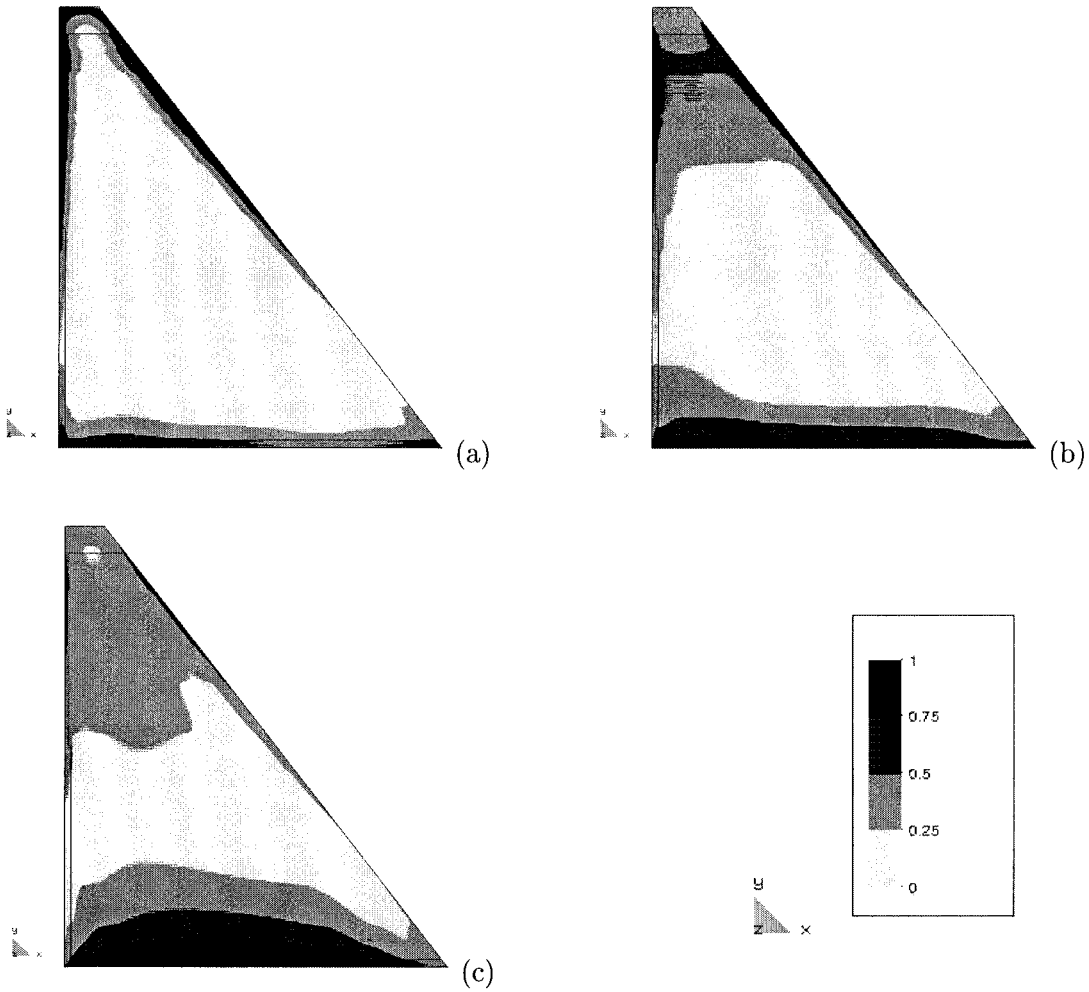

FIG. 6. Long-Term Evolution of Tensile Ratio; Winter Distribution for: (a) 1989; (b) 1991; (c) 1999

correctly evaluated by the designers of Urugua-í Dam, and they provided transverse contraction joints every 70–90 m above Elevation 182 m.

Fig. 5 shows contour plots for the evolution of the tensile ratio in the body of the dam during the construction process (1 year). The corresponding (months) elevations are (June 1988) 146 m, (November 1988) 175 m, and (June 1989) 196 m [Figs. 5(a–c), respectively]. As mentioned above, the developed stresses in the dam interior are initially compressive because they are due to the increase of temperature due to the hydration heat; they turn into tension some months after the concrete is placed, when the release of heat is completed and the concrete has started to cool. During this first year, tensile stresses develop mainly in the lower part of the dam, because of external restraint caused by the foundation, and at the upstream and downstream faces, because of the restraint against environmental thermal variations. Due to the low thermal conductivity of concrete, temperature gradients due to the difference between the ambient and inside temperatures are limited to a distance of about 2 m from the exterior faces. To avoid superficial cracking induced by these temperature gradients transverse contraction joints are cut in the facing of the dam every 14.24 m (1.20-m deep and running inside the RCC).

Fig. 6 shows contour plots for the evolution of the tensile ratio in the body of the dam during the first 11 years after dam completion. All of the snapshots correspond to the temperature distribution in the winter (June). The corresponding years are 1989, 1991, and 1999 [Figs. 6(a–c), respectively]. Note how, as the overall temperature in the dam decreases, thermally induced tensile stresses progressively develop due to internal and external restraint. In the upper part of the dam they are due to the internal restraint provided by the warmer concrete below; in the lower part of the dam free volume changes are restricted by the warmer concrete above and the cooler foundation rock below. The risk of cracking in the upper part of the dam is larger in the first 2 years after completion. Later, temperature becomes more uniform, and the phenomenon of internal restraint is less significant.

Interruption of Construction Process

The complete stress analysis is repeated now considering that there is an interruption of the construction process during the winter months due, for instance, to inadequate weather conditions or flooding of the construction site. Thus, the concreting schedule from January until the end of June 1988 is followed as for the reference case; then it is stopped during July, August, and September and resumed at the same placing speed from the beginning of October 1988 until the end of June 1989.

Fig. 7 shows the temperature evolution for interior points located at different elevations. The corresponding (placing month) elevations are as follows: (4) 130 m, (5) 135 m, (6) 141 m, (10) 147 m, (11) 153 m, (12) 159 m, (1) 165 m, (2) 171 m, (3) 177 m, (4) 181 m, and (5) 185 m. Note the interruption during the winter, months 7 to 9. Higher temperature rises appear at the bottom lifts (April to June), because of the heat coming from the hydration of the H180 concrete in the foundation and in the lifts placed during the austral summer (December to February). The temperature is still rising in most

of the dam after completion, particularly in those lifts placed immediately before and after the winter interruption (June and October). The bottom layers, however, start to cool shortly after being placed because of the heat conduction toward the founding rock. Compared to the short-term temperature evolution for the reference case (see Part I), it can be observed that higher temperatures are attained in the middle part of the dam, between elevations 150 and 170 m, while lower temperatures arise above the latter elevation.

Fig. 8 shows the long-term evolution of the tensile ratio for five of these interior points. This has to be compared with Fig. 4 to evaluate the influence of the interruption in the construction program. The risk of cracking at the lower elevations due to external restraint is mostly unaltered by the interruption; however, it is quite evident that the risk of cracking due to internal restraint has increased significantly, particularly for elevations above 150 m. Note that tensile stresses are still increasing after 12 years in most of the dam body. To ensure the same level of safety as for the reference case, in this situation transverse contraction joints should be provided every 70–90 m above Elevation 150 m at least, and not above Elevation 182 m, as in the actual design of the dam.

Fig. 9 shows contour plots for the evolution of the tensile ratio in the body of the dam during the first 10 years after completion of the dam. All of the snapshots correspond to the temperature distribution in the winter (June). The corresponding years are 1989, 1991, and 1999 [Figs. 9(a–c), respectively]. This has to be compared with Fig. 6 to evaluate the influence of the interruption in the construction program. Again, it can be observed how thermally induced tensile stresses progressively develop as the overall temperature decreases. Now, the higher risk of tensile cracking occurs in the upper middle part of the dam, between elevations 160 and 180 m. The risk of cracking in the middle part of the dam continues to grow even 10 years after completion. Note also how, in Fig. 9(c), the elevation at which the interruption took place is clearly visible.

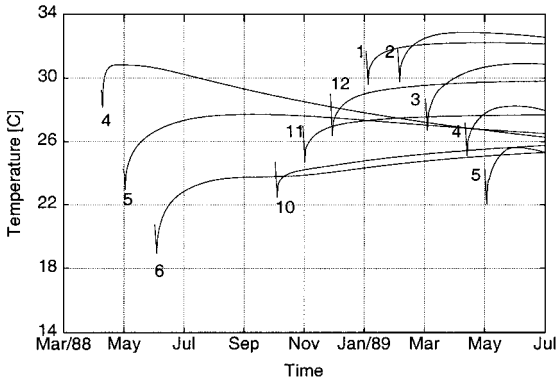

FIG. 7. Temperature Evolution for Different Elevations with 3-Month Interruption

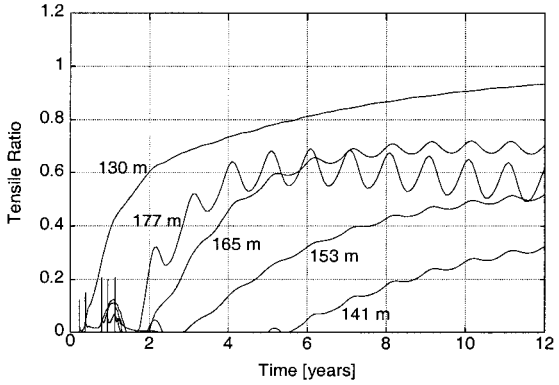

FIG. 8. Long-Term Tensile Ratio Evolution for Different Elevations with 3-Month Interruption

Slowing of Construction Process

Finally, the complete stress analysis is repeated considering that the placing interval is doubled to 96 h, that is, one 40-cm-thick lift is placed every 4 days. Therefore, the placing speed can be estimated as $V = 10$ cm/day. Now, RCC placing begins in April 1988 and finishes in December 1989. The spillway is cast in H220 from January to February 1990.

Fig. 10 shows the temperature evolution for interior points located at different elevations. The corresponding (placing month) elevations are as follows: (4) 130 m, (5) 135 m, (7) 141 m, (9) 147 m, (11) 153 m, (1) 159 m, (3) 165 m, (5) 171 m, (7) 177 m, and (9) 185 m. As in the previous cases, higher temperature rises appear at the bottom lifts (April to June) and in the lifts placed during the austral summer (December to February). Compared to the short-term temperature evolution for the reference case (see Part I), it can be observed that higher temperatures are attained in the middle part of the dam, between Elevations 150 and 170 m, whereas lower temperatures arise below and above these elevations. Because of the doubled duration of the construction process, heat conduction plays a more significant role in this case than in the ones analyzed previously; the bottom part of the dam attains higher temperatures than in the reference case due to heat flowing from the middle part, and, reciprocally, the middle part begins to cool quite rapidly due to heat flowing down and upward.

Fig. 11 shows the long-term evolution of the tensile ratio for five of these interior points. This has to be compared with Fig. 4 to evaluate the influence of the slowing in the construction program. It is quite evident that the risk of cracking due to internal restraint has increased significantly in the middle part of the dam, placed during the summer (see curves for Elevations 153 and 165 m). On the other hand, tensile stresses are reduced in the upper part of the dam, placed in colder weather than in the reference case; stress at Elevation 177 m, for instance, is very much reduced, and it follows nicely the regular seasonal oscillations. To ensure the same level of safety as for the reference case, in this situation transverse contraction joints should be provided every 70–90 m above Elevation 150 m at least and not above Elevation 182 m as in the actual design of the dam.

Fig. 12 shows contour plots for the evolution of the tensile ratio in the body of the dam during the first 10 years after completion of the dam. All of the snapshots correspond to the temperature distribution in the winter (June). The corresponding years are 1990, 1992, and 2000 [Figs. 12(a–c), respectively]. This has to be compared with Fig. 6 to evaluate the influence of the slowing in the construction program. It is clear that concreting in hot weather leaves its mark in the long-term mechanical behavior of the dam. Now, the higher risk of tensile cracking occurs in the middle part of the dam, between Elevations 150 and 170 m. The risk of cracking in the middle part of the dam is noticeable only 1 year after completion of the dam, and it continues to grow steadily even 10 years after completion.

CONCLUSIONS

This work presents a numerical procedure to simulate the stress analysis of the evolutionary construction process of RCC dams. The proposed procedure is used to perform the corresponding thermomechanical analysis of Urugua-í RCC Dam, in Argentina. Results obtained from the performed simulations using 2D models suggest the following conclusions:

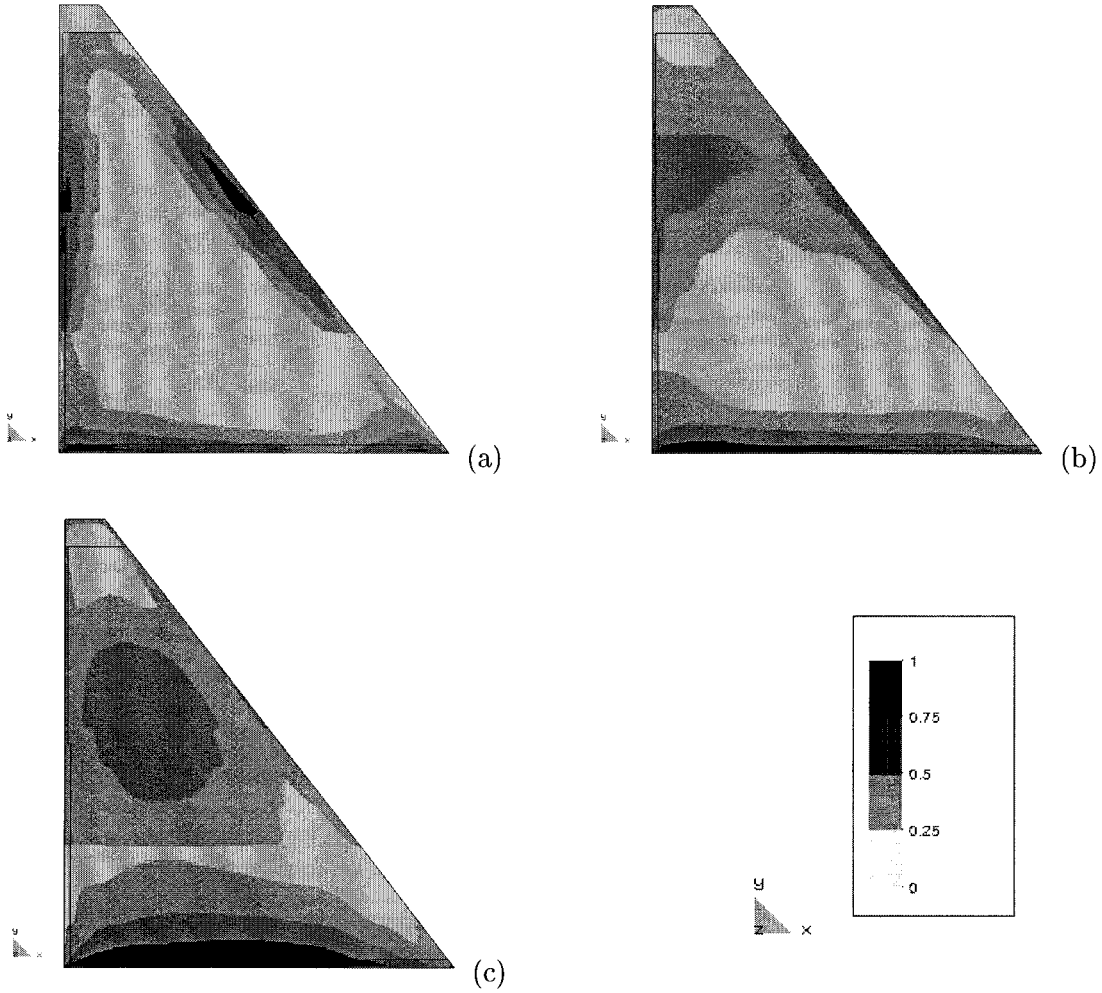

FIG. 9. Long-Term Evolution of Tensile Ratio with 3-Month Interruption; Winter Distribution for: (a) 1989; (b) 1991; (c) 1999

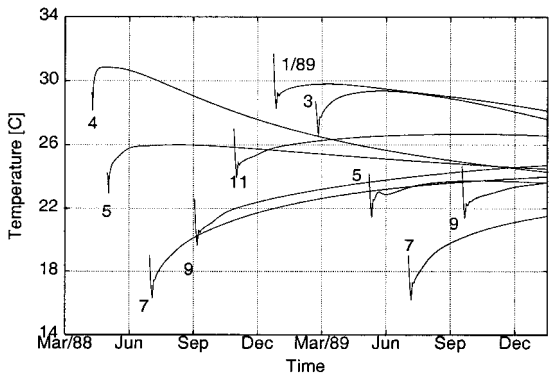

FIG. 10. Temperature Evolution for Different Elevations Slowing Construction Process

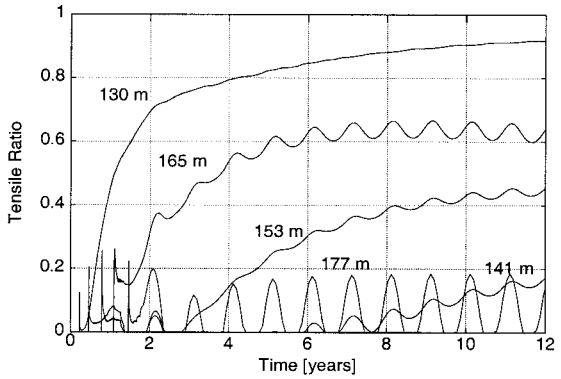

FIG. 11. Long-Term Tensile Ratio Evolution for Different Elevations Slowing Construction Process

- The proposed procedure is able to predict the evolution in time of the thermally induced tensile stresses that develop due to hydration heat released during the construction and the subsequent cooling process; this allows one to assess the risk of occurrence of tensile damage either at short or long term.
- The stress field inside the dam can be computed at any time during the construction process, and more importantly, during the first years following the completion of the dam, while the temperature in the dam body decreases to reach the final stable distribution.
- Results from the reference analysis, reproducing the actual conditions of the construction of Urugua-í Dam, show that significant tensile stresses develop in the bottom part of the dam due to the external restraint imposed by the foundation rock and also in the top part of the dam due to the internal restraint imposed by the concrete below, especially in the lifts placed during the austral summer (December to February). The latter was correctly evaluated by the designers of Urugua-í Dam, as they provided transverse contraction joints every 70–90 m above Elevation 182 m.
- The impact of a 3-month interruption of the construction process during the winter due, for instance, to inadequate weather conditions or flooding of the construction site has been considered. It turns out that in such a case transverse contraction should be cut deeper inside the dam, from

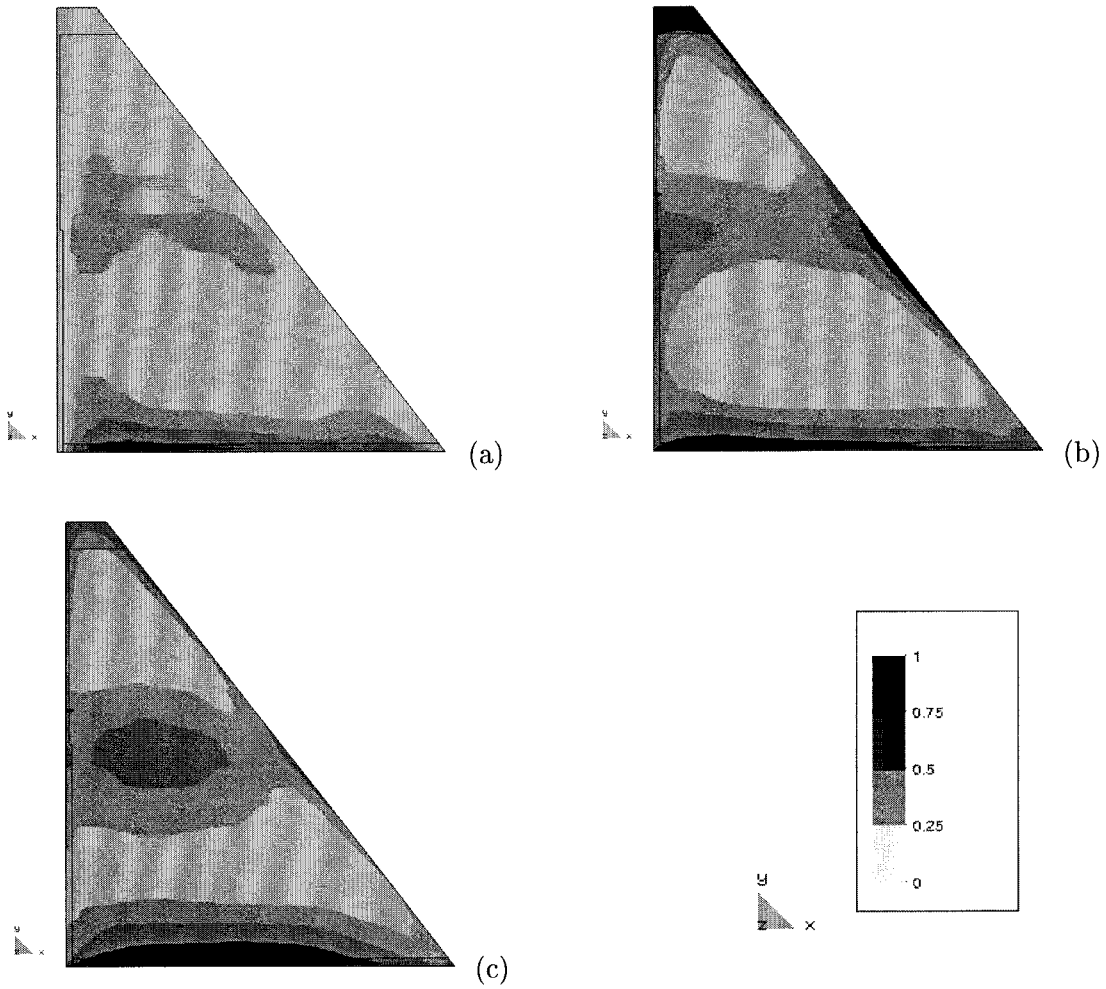

FIG. 12. Long-Term Evolution of Tensile Ratio Slowing Construction Process; Winter Distribution for: (a) 1990; (b) 1992; (c) 2000

Elevation 160 at least, to provide the same level of safety against cracking. The risk of cracking due to the external restraint of the foundation remains unaffected.

- An alternative placing schedule, with the placement interval doubled and the construction process completed in 2 years, was also considered. It turns out that heat conduction during construction plays a significant role in this case; transverse contraction joints should also be cut deeper inside the dam for this case, from Elevation 150 at least, to provide the same level of safety against cracking.

APPENDIX I. REFERENCES

Bazant, Z. P. (1979). ''Thermodynamics of solidifying or melting viscoelastic material.'' *J. Engrg. Mech. Div.*, ASCE, 105(6), 933–952.

Bazant, Z. P., Hauggard, A. B., Baweja, S., and Ulm, F. J. (1997). ''Microprestress-solidification theory for concrete creep. I: Aging and drying effects.'' *J. Engrg. Mech.*, ASCE, 123(11), 1188–1194.

Bazant, Z. P., and Prasannan, S. (1989). ''Solidification theory for concrete creep. I: Formulation.'' *J. Engrg. Mech.*, ASCE, 115(8), 1691–1703.

Carol, I., and Bazant, Z. P. (1993). ''Viscoelasticity with aging caused by solidification of nonaging constituent.'' *J. Engrg. Mech.*, ASCE, 119(11), 2252–2269.

Cervera, M., Oliver, J., and Prato, T. (1999). ''Thermo-chemo-mechanical model for concrete. II: Damage and creep.'' *J. Engrg. Mech.*, ASCE, 125(9), 1028–1039.

Cervera, M., Oliver, J., and Prato, T. (2000). ''Simulation of construction of RCC dams. I: Temperature and aging.'' *J. Struct. Engrg.*, ASCE, 126(9), 1053–1061.

Fujisawa, T., and Nagayama, I. (1985). ''Cause and control of cracks by thermal stress in concrete dams.'' *Proc., 15th Congr. on Large Dams*, ICOLD, ed., Vol. 2, 117–143.

Hirose, T., Nagayama, I., Takemura, K., and Sato, H. (1988). ''A study on control temperature cracks in large roller compacted concrete dams.'' *Proc., 16th Congr. on Large Dams*, ICOLD, ed., Vol. 3, 119–135.

Widmann, R. (1985). ''How to avoid thermal cracking of mass concrete.'' *Proc., 15th Congr. on Large Dams*, ICOLD, ed., Vol. 2, 263–277.

APPENDIX II. NOTATION

The following symbols are used in this paper:

$\mathbf{D}^i$ = elastic constitutive tensor for Maxwell element i;
d^+, d^- = tensile and compressive damage indices, respectively;
E^i, E^i_∞ = elastic modulus for Maxwell element i and final value, respectively;
T, T_{ref} = temperature and reference temperature, respectively;
t = time;
α_T = thermal expansion coefficient;
$\boldsymbol{\varepsilon}$ = strain tensor;
$\boldsymbol{\varepsilon}^i_e$, $\boldsymbol{\varepsilon}^i$ = elastic and viscous strain tensors for Maxwell element i, respectively;
$\boldsymbol{\varepsilon}_T$ = thermal strain tensor;
κ = aging degree;
ξ_{set} = hydration degree at setting;
$\boldsymbol{\sigma}$, $\bar{\boldsymbol{\sigma}}$ = stress tensor and elastic stress tensor, respectively;
τ_a = relaxation time associated to aging;
τ^i = relaxation time for Maxwell element i;
τ_μ = relaxation time associated to flow term;
$\mathbf{1}$ = unit (second-order) tensor; and
$(\dot{})$ = time derivative or rate.